Dielectric relaxation and molecular motion in comb-shaped liquid crystal polymers

J. P. Parneix[a]; R. Njeumo[a]; C. Legrand[a]; P. Le Barny[b]; J. C. Dubois[b]

[a] Centre Hyperfréquences et Semiconducteurs, U.A. C.N.R.S. 287, Université de Lille I, Flandres Artois, Villeneuve d'Ascq Cedex, France [b] Laboratoire Central de Recherches, Thomson-CSF, Domaine de Corbeville, B.P. 10, 91400, Orsay Cedex, France

PLEASE SCROLL DOWN FOR ARTICLE

Dielectric relaxation and molecular motion in comb-shaped liquid crystal polymers

by J. P. PARNEIX†, R. NJEUMO†, C. LEGRAND†, P. LE BARNY‡
and J. C. DUBOIS‡

†Centre Hyperfréquences et Semiconducteurs, U.A. C.N.R.S. 287, Université de
Lille I, Flandres Artois, 59655 Villeneuve d'Ascq Cedex, France

‡Laboratoire Central de Recherches, Thomson-CSF, Domaine de Corbeville,
B.P. 10, 91400 Orsay Cedex, France

Dielectric studies have been performed on a series of oriented polyacrylates in broad frequency and temperature ranges, 5 Hz to 1 GHz and $-170°C$, to $+200°C$ respectively. In order to assist in the identification of the observed relaxation mechanisms, different molecular structures of the mesogenic pendant group connected to the main chain via a variable intermediate group have been investigated. The influence of the intermediate group (spacer length n), of the central group (O or COO), of the interphenyl group (COO) as well as that of the terminal group (CN or OCH_3), upon the nature of the relaxations (α, β, γ or δ) and the critical times of the molecular dynamics in side-chain liquid crystal polymers are discussed separately.

1. Introduction

Polymeric liquid crystals involving a mesogenic group in the side-chain are objects of increasing interest. They combine the properties of low molecular weight liquid crystals with those of polymers, which yield a large range of potential applications [1, 2]. Although it has been well documented that the dielectric method is an efficient one for studying the molecular dynamics of polymers [3, 4], its utilization for the investigation of liquid-crystalline polymers has begun only recently [5–7]. The aims of the present work are both to widen the frequency and temperature ranges of investigation and to study various molecular structures, in order to assist in the identification of the observed relaxation processes and assign them to the motion of different parts of the molecule, with a better accuracy. The samples can be oriented in the mesomorphic phases, which allows some relaxation processes to be enhanced and hence, to identify them better. Furthermore, the determination of the anisotropy in the static permittivity ($\Delta\varepsilon' = \varepsilon'_{\parallel} - \varepsilon'_{\perp}$) is of greater interest for applications.

Comparative studies were carried out on compounds with the structural formulae shown in table 1; all of these compounds were synthesized at LCR Thomson CSF by P. Le Barny. The phase transitions were studied by D.S.C. and polarizing microscopy and the phase structure by X-ray diffraction [9]. The influence of four parameters upon the nature of the relaxation mechanisms and the critical times of the molecular dynamics in these compounds are discussed separately. These parameters are (a) the intermediate group (spacer length n); (b) the central (O or COO) group; (c) the interphenyl (COO) group; and (d) the terminal (CN or OCH_3) group.

Table 1.

Structural formula

$$-(CH_2 - CH)_x -$$

$$\underset{O}{\overset{}{\diagup}}\overset{C}{\underset{O-(CH_2)_n}{\diagdown}}\!-\!X\!-\!\boxed{O}\!-\!Y\!-\!\boxed{O}\!-\!Z$$

Sample code	Spacer length (n)	Transition temperatures (in °C)	X	Y	Z
SSP2F1	2	G 84 'N' order 113·5 I	O	–	CN
PLBP24	3	G 54 ? 60 S_{A_d} 82 I	O	–	CN
PLBP25	4	G 42 N 110 I	O	–	CN
PLBP14	5	G 53 ? 75 S_{A_d} 120 N 124·4 I	O	–	CN
PLBP12	6	G 32 N_{Re} 80 S_{A_d} 124·5 N 132 I	O	–	CN
LMWLC [10]	–	C 53·8 S_{Ad} 65·6 N 78·4 I	O	–	CN
PLBP10	5	G 30 N 115 I	COO	–	CN
LMWLC [10]	–	C 42·5 S_A 63 N 76 I	COO	–	CN
PLBP29	6	G 22·5 N 106 I	O	COO	CN
LMWLC [13 (b)]	–	C 44·6 N 59.6 I	–	COO	CN
PLBP30	6	G 17·5 S 82 N 100 I	O	COO	OCH_3

2. Experimental section

The samples were investigated in their isotropic, mesomorphic and glassy states (except for very viscous samples SSP2F1 and PLBP24) with the aid of the experimental technique described previously [8 (*a*)]; the equipment consists of three parts:

(1) The measurement devices are two Hewlett-Packard impedance analysers HP 4192 A (5 Hz to 13 MHz) and HP 4191 A (1 MHz to 1 GHz), piloted by a HP 87 computer. They allow automatic measurements of the complex permittivity [$\varepsilon^*(\omega) = \varepsilon'(\omega) - i\varepsilon''(\omega)$] of the sample to be made that can be easily stored or plotted. In the whole frequency range, more than 20 measurement points per decade can be obtained. The static permittivities were obtained at a frequency F_0, low enough to prevent dispersion mechanisms and high enough to avoid the influence of conductivity. When this is too large, because of the effect of temperature, the static permittivity is obtained by prolonging the dispersion domain (conductivity is deduced). The dielectric relaxation spectra display the plots $\varepsilon'(f)$, $\varepsilon''(f)$ and the Cole–Cole diagram $\varepsilon''(\varepsilon')$ (with temperature as a parameter).

(2) The experimental cell is a parallel plate capacitor located at the end of a coaxial line. The sample is introduced into the free interelectrode volume by using capillary filling. The necessary sample volume is smaller than 10 mm^3. This cell makes it possible to study the two main orientations of the director ($E \parallel n$ or $E \perp n$) in various mesomorphic phases.
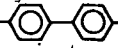
(3) Additional apparatus to this set-up is a strong electromagnet, a temperature regulator and a system providing an inert nitrogen atmosphere that prevents, in some cases, sample degradation, especially when working in the higher temperature range. The orientation of the optic axis (n) of the sample was achieved by slowly cooling the cell from the isotropic phase under a magnetic field of 1·2 T, provided by the electromagnet. Such a field is known to be capable of orientating the optic axis of a

nematogen 100 μm thick [8 (b)]. To check this orientation, we measured the dielectric constants as a function of the applied magnetic field (with temperature as a parameter). The curves converge to saturation values (different in each orientation of the director), which we took as the fully oriented values. In such cases, if there appears no anomaly in the dielectric spectra in the parallel measurement direction (a Debye type curve is expected), we assume that the sample is well orientated. The temperature was regulated from room temperature to 230°C by using a Eurotherm programmable thermal regulator EI 822; this provides an accuracy of 0·4°C with a set point of 200°C and with better accuracy at lower temperatures. A home-made regulator based on forced circulation of liquid nitrogen was used for measurement from room temperature to − 170°C.

3. Results and discussion
3.1. *Influence of the spacer length (n)*
3.1.1. *Static*

Figure 1 shows the variation of the static permittivity versus temperature for all the compounds. We note that the data in the mesomorphic phases are reported only for spacer lengths $n \geqslant 4$. This is due to the difficulty of orientating the optic axis of the sample for shorter spacers $n = 2$ or 3; indeed, they lead to extremely viscous samples. In figure 1 the variation of the permittivity of the low molecular weight liquid crystal of the same chemical structure as the mesogenic pendant group $(C_8H_{17}O-\bigcirc-\bigcirc-CN)$ are shown by a dotted line. In all cases, the static permittivity anisotropy is strongly positive ($\Delta\varepsilon' \sim 7\cdot5$). This relatively high value of $\Delta\varepsilon'$ is connected with the strong polar cyano terminal group. The apparent dipole moment was found to be much smaller than the effective dipole moment of an isolated molecule and the Kirkwood–Frohlich correlation factor $g = \mu_{app}^2/\mu_{isol}^2$ much smaller than 1 (Here, μ_{app} is the apparent dipole moment deduced, for example, in the isotropic phase from the Onsager equation; μ_{isol} is the dipole moment of an isolated molecule deduced from dilution measurements in non-polar solvents, extrapolated to infinite dilution [4 (c)].)
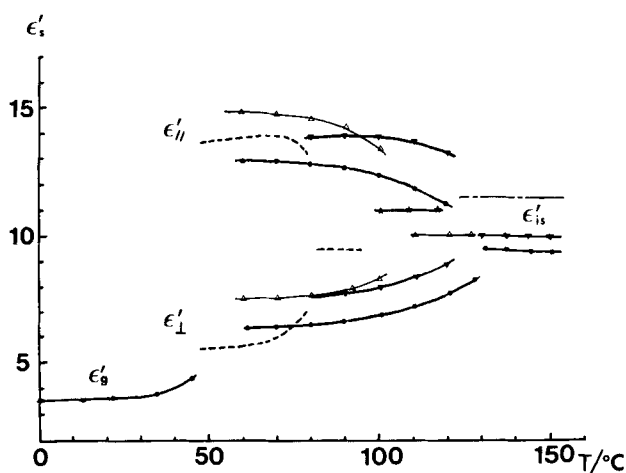

Figure 1. Variation of the static permittivity against temperature in the isotropic and meso-morphic ($E \parallel n$ and $E \perp n$) phases, for spacer length $n = 2 (-\cdot-)$; $n = 3 (\bigstar)$; $n = 4 (\triangle)$; $n = 5 (\blacktriangle)$; $n = 6 (\bullet)$ and for the low molecular weight liquid crystal $(---)$.

This observation can be explained by an antiparallel orientation of neighbouring pendant chains. This behaviour, observed in low molecular weight liquid crystals [11] also results in an increase of $\varepsilon'_\perp$ with increasing temperature. This result has been confirmed by X-ray diffraction studies [9]. At the glass transition, the permittivities decrease substantially implying that they are undergoing relaxation in the very low frequency range (i.e. lower than the low frequency limit of 5 Hz for the apparatus). At temperatures close to $-170°C$, they do not vary with frequency, which allows us to suppose that all the motions are frozen. Here, ε' (5 Hz) was found to be equal to 2·8.

3.1.2. *Dynamic*

The dielectric spectra in the isotropic and mesomorphic phases for the polymers of the series in table 1 ($X = O$, $Y = -$ and $Z = CN$, $n = 2$ to 6), show a similar behaviour (the observed loss processes exhibit a Debye behaviour in the low frequency range, but are slightly distributed at higher frequencies for all the samples). For this reason we shall give the results only for polymer PLBP12 which presents the richest polymorphism of all, more particularly a re-entrant nematic phase that will be characterized completely.
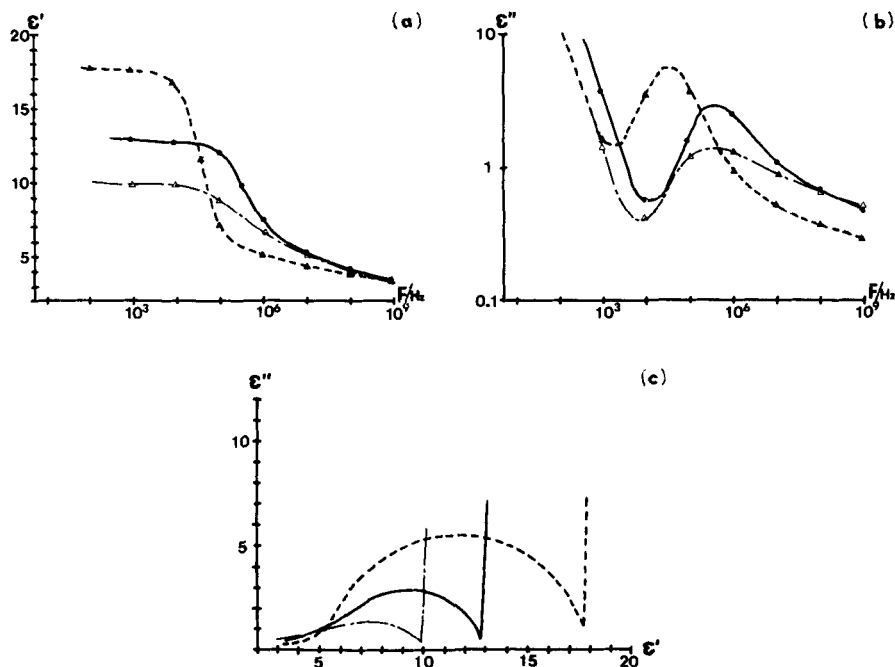

Figure 2.   Real (*a*) and imaginary (*b*) part of the complex permittivity against frequency for polymer PLBP12; The Cole–Cole diagram (*c*). ●, isotropic (135°C); ▲, mesomorphic $E \parallel n$ (120°C); △, mesomorphic $E \perp n$ (120°C). 20 measurement points per decade (only a few points are shown in order not to congest the figures).

Isotropic phase

The spectra in this phase were obtainable for all the samples. Figure 2 shows the variation of the dielectric permittivity ε' and the dielectric loss factor ε'' as a function of frequency at a given temperature. The critical frequency (F_c) related to this loss process corresponds with the maximum of ε'', and the energy barrier for dipole
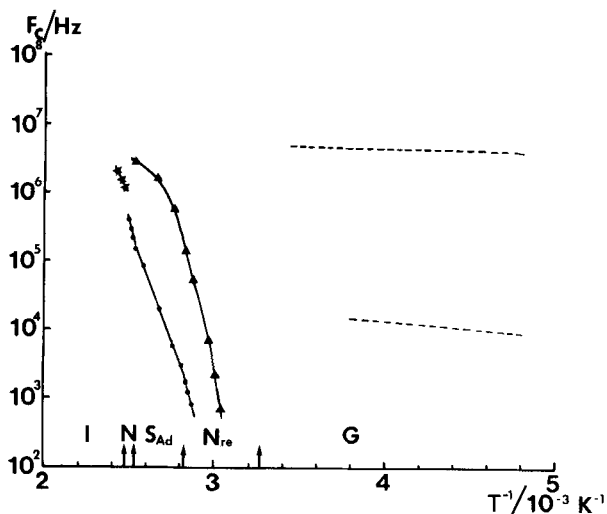
Figure 3. Critical frequency versus the reciprocal of temperature for polymer PLBP12 ($n = 6$), ★, iso; ●, $E \parallel n$; ▲, $E \perp n$; – – –, are related to very low losses in the glassy phase; the values are qualitative only (large uncertainties).

relaxation, W, is determined from the plots of $\log(F_c)$ versus reciprocal temperature (see figure 3), by assuming an Arrhenius type law

$$F_c = F_0 \exp(-W/kT).$$

Figure 4 shows the variations of F_c (at a reduced temperature, T/T_{NI}, of 1·1) and W against the spacer length (n). We note that F_c increases and W decreases with increasing n, which indicates a larger mobility of the side-chain.

Mesomorphic phases

$E \parallel n$. When the electric field is parallel to the director ($E \parallel n$), the Cole–Cole plots show Debye-type loss processes, very slightly distributed at higher frequencies (see figure 2). Similar behaviour is always observed for low molecular weight liquid crystals [10, 11]. It is characteristic of a single molecular mechanism which can be attributed to the reorientational motion of the molecules around an axis perpendicular to their longitudinal axis. For polymers this kind of motion is no longer possible because of the presence of the spacer. The relaxation process is assigned to the rotation of the side-group about the polymer backbone [5, 12]. A re-entrant nematic phase (N_{Re}) was recently discovered in polymer PLBP12 [9]. This situation led us to perform accurate measurements (every 0·5°C) in the vicinity of the N–S_A phase transition, and to study the δ relaxation in the N_{Re} phase. The variation of the critical frequencies of the loss process observed in this direction are plotted versus reciprocal temperature in figure 3. The data allow the calculation of the activation energy (Arrhenius law), which leads to the values listed in table 2 (the energies for the low molecular weight liquid crystals having the same chemical structure as the pendant chain are also reported there). The following relations can be deduced from these results $F_c(\text{PLC}) \sim (1/10^{-3}) F_c(\text{LMWLC})$; $W(\text{PLC}) \sim 2W(\text{LMWLC})$; $W_{N_{Re}} > W_N > W_{S_A}$; here PLC denotes the polymeric species and LMWLC the low molecular weight mesogens. The last inequalities have also been observed in low molecular weight liquid crystals [13 (a)].
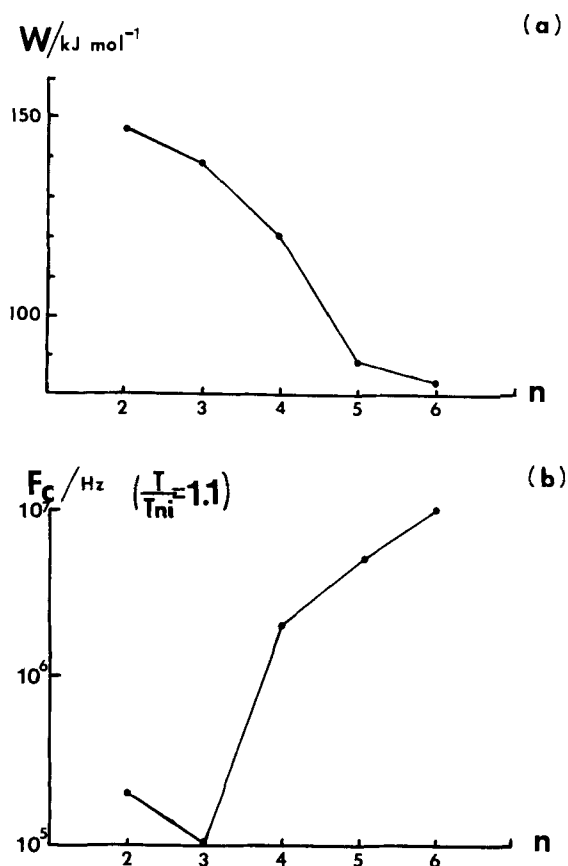
Figure 4. (*a*) Activation energies, W, against spacer length, n, in the isotropic phase of polymers listed in table 1 (the first five, $n = 2$ to 6). (*b*) Critical frequency of the domain observed in the isotropic phase against the spacer length n (for the same samples at $T = 1 \cdot 1 T_{NI}$).

Table 2.

Sample code	Phase sequence Spacer length, n	N_{Re}	S_{A_d} Energies/kJ mol^{-1} $E \parallel n$	N	I
SSP2F1	2	—	—	—	147
PLBP24	3	—	—	—	138
PLBP25	4	—	—	177	120
PLBP14	5	—	—	131	88
PLBP12	6	241	126	193	83
LMWLC [10]	—	—	48	73	—
PLBP10	5 + COO	—	—	143	61
LMWLC [10]	—	—	46	70	—
PLBP29	6	—	—	149	110
LMWLC [13 (b)]	—	—	—	85	46
PLBP30	6	—	83	163	88

$E \perp n$. One example of the spectra obtained in the perpendicular measurement direction ($E \perp n$) is given in figure 2. The Cole–Cole plot is strongly distributed and could be related to the co-existence of several relaxation mechanisms [13], such as the libration of the CN group and intramolecular rotations. Indeed, this plot is analogous to those observed for low molecular weight mesogens but the critical frequencies are three orders of magnitude lower. In fact this relaxation can be explained differently. The variations of F_c of the flat domain observed for this director orientation versus T^{-1} are fitted by the Arrhenius equation (see figure 3). The plot is curved and its prolongation cross the abscissa at T_g^{-1}. It has been shown [12(a)] that the glass transition is strongly affected by the interaction between the mesogenic groups and that this type of plot characterizes the dynamic glass process [14] represented by the α relaxation. The transverse component of the dipole moment of the mesogenic head group is the source of this relaxation [12(c)]. The amplitude of this process is relatively small ($\varepsilon''_{max} = 0.8$) in comparison to that of the δ relaxation ($\varepsilon''_{max} = 4$). This is the reason why the α process is well displayed in the perpendicular director alignment, where the δ process does not exist.

Glassy phase

Below the glass transition temperature T_g, two different relaxation processes are observed; they are located in the kilohertz and megahertz ranges respectively. Figure 5 (*b*) displays the variations of the di-electric loss factor ε'' versus frequency for polymer PLBP12. We note that dielectric losses decrease with decreasing temperature for the high frequency loss process and has the opposite behaviour for the low frequency loss process.

We wish to remark that the accuracy is better for ε' than for ε'', due to very small losses. Consequently, F_c must be taken from the curves $\varepsilon'(f)$ (figure 5 (*a*)) which leads to a larger uncertainty in the location of F_c (the corresponding points are indicated by a dotted line in figure 3).

The higher frequency range process is related to the libration of the terminal cyano group, we shall call it the γ_1 relaxation. The frequency range of this libration is about 100 times lower than that observed for small molecules [10]. The second mechanism in the lower frequency range is a very slow process ($F_c \sim 10\,\mathrm{kHz}$) that varies very
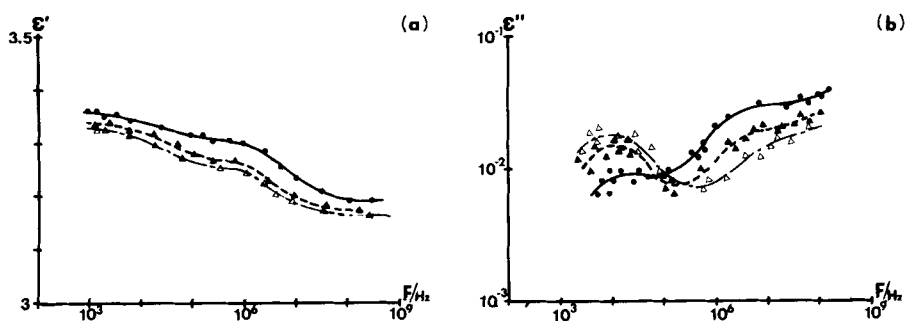

Figure 5. Real (*a*) and imaginary (*b*) part of the complex permittivity versus frequency for polymer PLBP12 in the glassy phase; $-30°C$ (●); $-52°C$ (▲); $-62°C$ (△). 20 measurement points per decade (the accuracy is better for ε' than for ε'').

slowly with temperature. It can be associated with the motion of the spacer; we shall call it the β relaxation.

In concluding this part, the following points can be recalled:

(*a*) The δ relaxation is related to the rotation of the whole side group around the polymer backbone. It is observed in the isotropic and mesomorphic ($E \parallel n$) phases.

(*b*) The α relaxation is related to the motion of the side group rigidly attached to the polymer main chain (main chain motion). This process is better observed in the perpendicular director alignment measurement, since it is no more absorbed by the large domain of the δ process.

(*c*) The β relaxation is connected with motion within the spacer.

(*d*) The γ_1 relaxation is a high frequency process related to the libration of the terminal cyano group. It was observed for all the polymers investigated. By varying the molecular structure of this group, the assignment of the γ_1 relaxation to the motion in this sequence will be demonstrated with a better accuracy. This will be done later in this work.

3.2. *Influence of the intermediate group*

In this paragraph a COO group replaces the O group of the series studied previously. The spacer length is kept constant with $n = 5$. The structural formulae of the polymers to be compared (PLBP10 and PLBP14) are given in table 1.

3.2.1. *Static*

In figure 6 we show the variation of the static permittivity, ε', as a function of temperature in the isotropic and mesomorphic phases for polymers PLBP14 and PLBP10 and for the low molecular weight liquid crystals having the same chemical formula as the mesogenic pendant group [10]. For all of them the dielectric anisotropy ($\Delta\varepsilon' = \varepsilon'_\parallel - \varepsilon'_\perp$) is strictly positive ($\Delta\varepsilon' \sim 7$) and there is no substantial change either in $\varepsilon'_\parallel$ or in $\varepsilon'_\perp$. The dipole moments of the alkyl–ether and alkyl–oxygen groups are
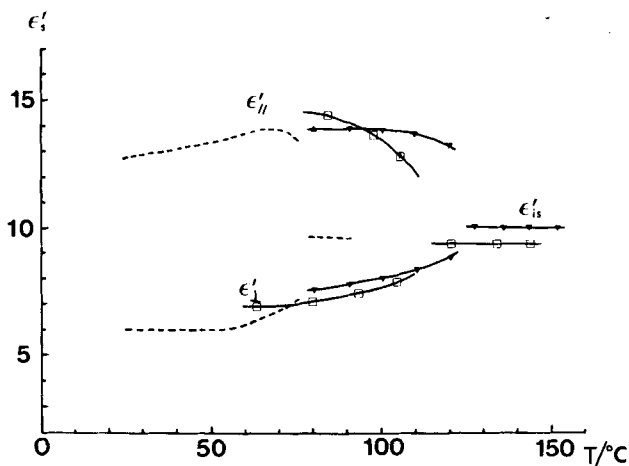

Figure 6. Variation of the static permittivity against temperature for polymer PLBP14 (▲) and PLBP10 (□) and for low molecular weight liquid crystals (– – –).

calculated from [15] and their components in a coordinate system with axes parallel and perpendicular to the line across the C aromatic–O bond are respectively (μ_l = 0.89 D; μ_t = 1.68 D) and (μ_l = 0.39 D; μ_t = 1.22 D); we conclude that the dipole moment induced by the presence of the COO group does not play a noticeable role. The behaviour of the whole side-chain is still governed by the strong polar cyano end group ($\mu_l \sim 4.05$ D) common to all of them.

3.2.2. *Dynamic*

Figure 7 shows the plots of the real (ε') and imaginary (ε'') parts of the complex permittivity versus frequency for polymer PLBP10 in different phases. As in the previous series, quasi and pure Debye-type curves are obtained in the isotropic and mesomorphic $E \parallel n$ phases respectively, in the low frequency range. When we plot the critical frequencies of the observed loss processes in all phases for both of the measurement directions of the director, we obtain the curves of figure 8.

$E \parallel n$. For polymer PLBP10, the results in this direction are similar to those of the previous series. The activation energies of the δ relaxation in the mesomorphic phases are deduced from the slopes of the straight lines (Arrhenius law) as before. The inequality $W_N > W_{iso}$ still holds (but see later).

$E \perp n$. When the electric field is perpendicular to the director the relaxation is displayed as in the previous series with a non-Arrhenius law in the higher temperature range. The prolongation of this curve in the lower frequency range converges to $1/T_g$.
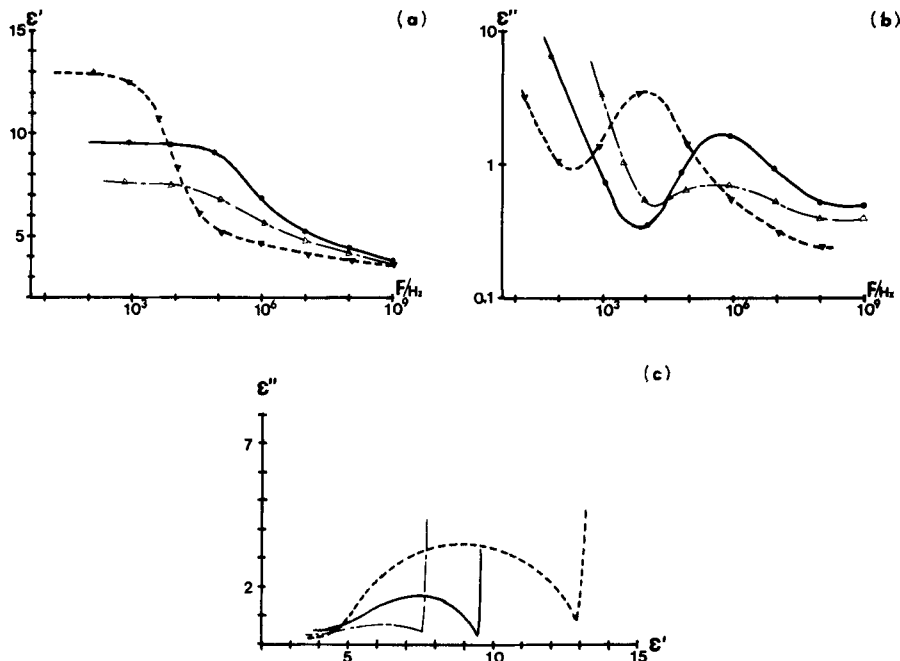

Figure 7. Real (*a*) and imaginary (*b*) parts of the complex permittivity versus frequency for polymer PLBP10 in the isotropic and mesomorphic phase; the Cole–Cole diagram (*c*); isotropic 129°C (●); mesomorphic 105°C $E \parallel n$ (▲); $E \perp n$ (△). 20 measurement points per decade (only a few points are shown in order not to congest the figures).
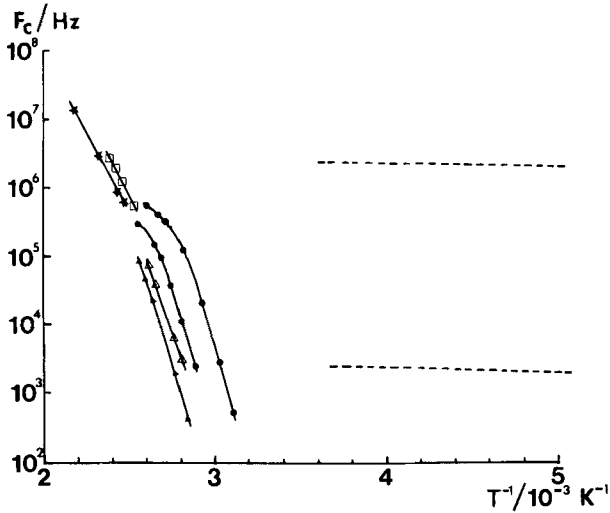
Figure 8.   Critical frequencies against T^{-1} for polymer PLBP14 iso ($\bigstar$); $E \perp n$ ($\bullet$); $E \parallel n$ ($\blacktriangle$), and polymer PLBP10 iso ($\square$); $E \perp n$ ($\circ$); $E \parallel n$ ($\triangle$) glassy (–––).

Below the glass transition temperature of polymer PLBP10, two different kinds of motions co-exist. They are characterized by their very small amplitudes ($\varepsilon''_{max} \sim 0.03$) and are located in the kilohertz and megahertz ranges respectively. Because of these very small losses, the location of the critical frequencies is not obvious. For this reason the dotted lines in figure 8 must be considered as qualitative only.

There is not any noticeable difference between the two polymers in the glassy phase and both of them should be discussed in the same way as in the previous series.

We note that at about 40°C above T_g, the δ relaxation is no longer displayed, since it is drowned in conductivity in the lower frequency range. A relaxation process which is probably connected with the α relaxation becomes active at this temperature in the higher frequency range. This was also observed in the previous series but with a lower amplitude, and also by other authors [12(c)].

3.3. *Influence of the central group*

Let us now consider the cases where a COO group is introduced between two phenyl rings. The polymer thus obtained (PLBP 29) is given in table 1.

3.3.1. *Static*

The variations of the static permittivities in both of the measurement directions for the director are shown in figure 9. The influence of the interphenyl COO group is striking and cannot be explained only by the increase of the resulting dipole moment, due to the introduction of this group. The static permittivities in the isotropic phase (ε'_{is}) and in the mesomorphic phase ($\varepsilon'_{\parallel}$ and $\varepsilon'_{\perp}$) vary rather strongly from one polymer to another. In particular, there appears a greater difference in the values of $\varepsilon'_{\parallel}$

$$\varepsilon'_{\parallel}(\text{PLBP12}) \sim 12; \quad \varepsilon'_{\parallel}(\text{PLB29}) \sim 19.$$

The values of the static anisotropies are

$$\Delta\varepsilon'(\text{PLBP12}) \sim 6{\cdot}5; \quad \Delta\varepsilon'(\text{PLBP29}) \sim 12.$$

The striking change in $\varepsilon'_\parallel$ and $\Delta\varepsilon'$ can result in an antiferroelectric decorrelation induced by the ester group.

A comparison with the behaviour of small molecules can be made using the results on the behaviour of the low molecular weight liquid crystal which has the closest structure as that in the mesogenic pendant group [13 (b)], where $\Delta\varepsilon'$ was found to be equal to 16.
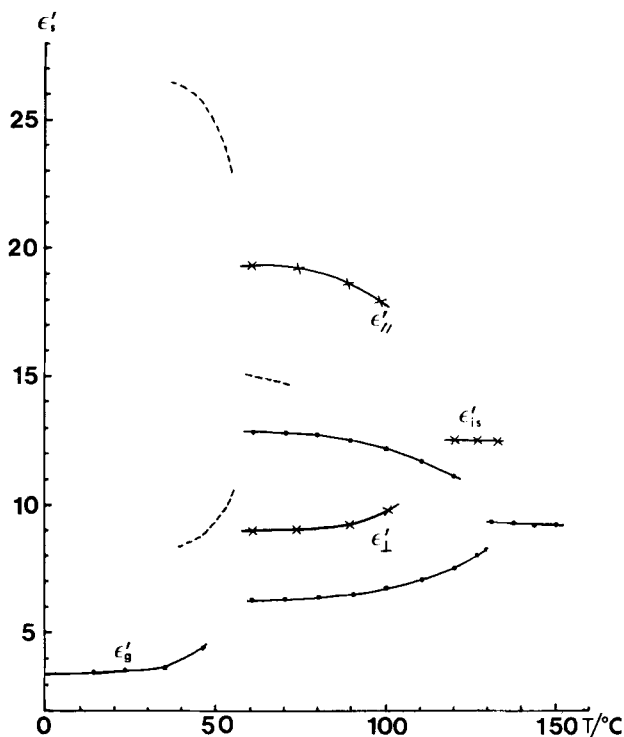

Figure 9. Comparative variations against temperature of the static permittivity for polymers PLBP12 (●), PLBP29 (×) and for the low molecular weight analogues of the pendant chain (−−−).

3.3.2. *Dynamic*

Figures 10 (a) and 10 (b) show the dielectric dispersion and losses respectively of polymer PLBP29 at various temperatures. In this case the curves are slightly less distributed than for PLBP12 (see figure 2). The resulting activation energies of the involved δ relaxation are given in table 2. In the perpendicular director alignment measurement the α relaxation is displayed as in the previous cases.

3.4. *Influence of the terminal group*

The samples under consideration in this part have the same structural formula and differ only in the terminal groups and phase sequences (see table 1, PLBP29 and PLBP30). The spacer length is chosen to be long enough to avoid viscosity problems and to allow performance of measurements in all mesophases in both of the main orientations of the director.
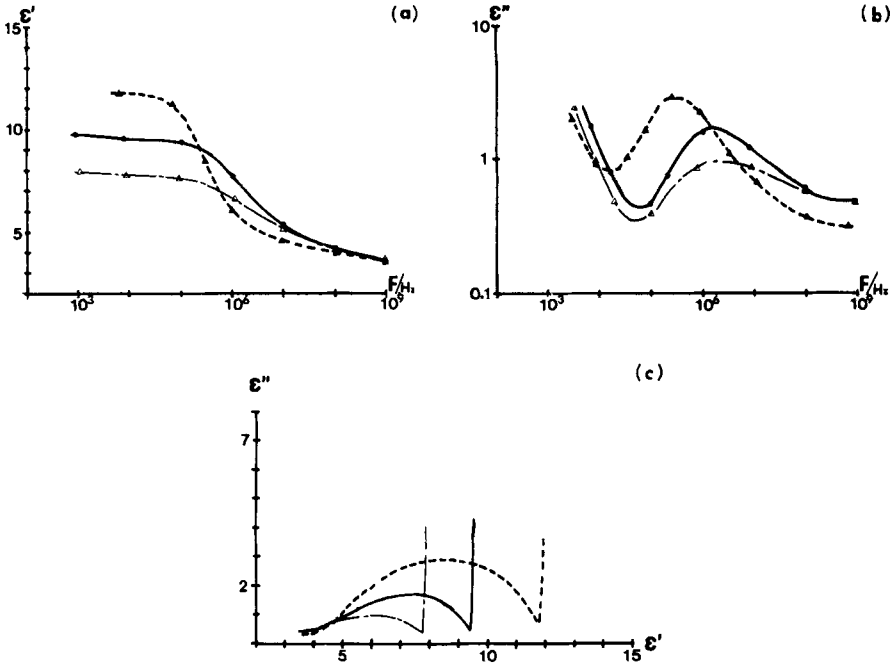
Figure 10.   Real (*a*) and imaginary (*b*) parts of the complex permittivity against frequency for polymer PLBP29; the Cole–Cole diagram (c). Isotropic phase (●): 115°C; nematic phase $E \parallel n$ (▲): 100°C; nematic phase $E \perp n$ (△): 100°C. 20 measurement points per decade (only a few points are shown in order not to congest the figures).

3.4.1. *Static*

The plots of $\varepsilon'_{\parallel}$ and $\varepsilon'_{\perp}$ versus temperature in the isotropic and mesomorphic phases of polymers PLBP30 are given in figure 11. The parallel component of the dipole moment of the OCH_3 group along the C (aromatic)–oxygen bond (μ_l) is about 10 times smaller than that of the CN group ($\mu_l \sim 4.05$ D), whereas the perpendicular component (μ_t) is much larger in the first case (1.22 D instead of 0 D) [15]. As a consequence, the static anisotropy $\Delta\varepsilon' (= \varepsilon'_{\parallel} - \varepsilon'_{\perp})$ is negative ($\Delta\varepsilon' \sim -2$).

3.4.2. *Dynamic*

Figure 12 shows the three characteristic curves [$\varepsilon'(f)$, $\varepsilon''(f)$ and $\varepsilon''(\varepsilon')$], obtained for polymer PLBP30 at various temperatures. The dynamic dispersion in the isotropic phase of PLBP30 displays two motions of the molecule, the first is of small amplitude ($\varepsilon''_{max} \sim 0.3$) and is located in the megahertz range; the second with a larger amplitude (0.8) is located in the gigahertz range. Since the two relaxation processes take place in the high frequency and high temperature ranges, they can be easily followed down to the glass transition temperature. The two polymers PLBP30 and PLBP29 differing in their terminal groups do not behave identically, since the dielectric dispersion diagrams of the former exhibit one more relaxation mechanism. The low frequency process is the δ relaxation described previously.

$E \parallel n$. When the electric field is parallel to the director, this process disappears at a temperature 40°C above T_g, drowned in conductivity, while a new process results,
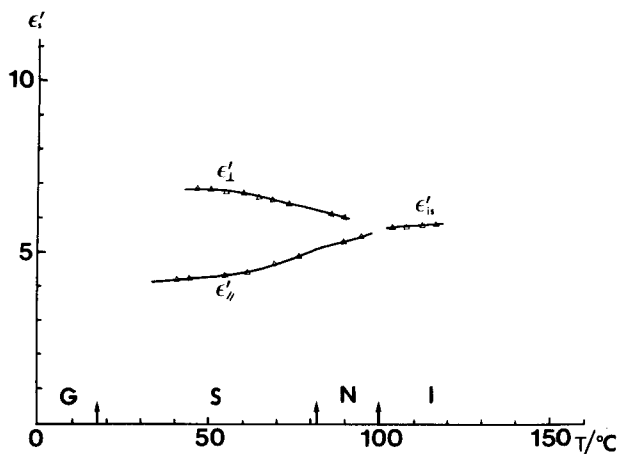
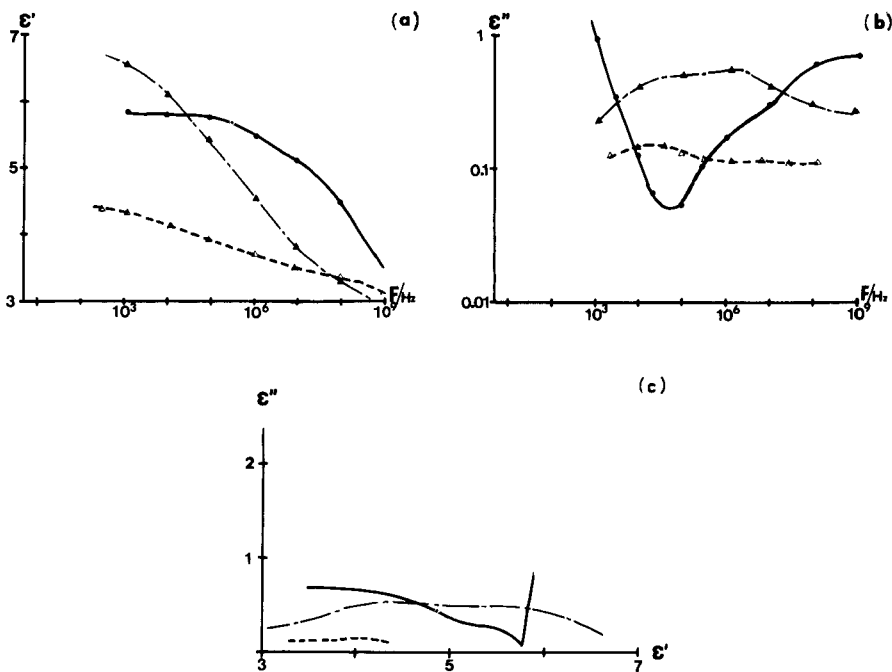Figure 11. Variations of the static permittivity against temperature in various phases of polymer PLBP30.

Figure 12. Real (*a*) and imaginary (*b*) parts of the complex permittivity versus frequency for polymer PLBP30 in the isotropic phase 116°C (●) and mesomorphic phase 47°C $E \parallel n$ (△); $E \perp n$ (▲). The Cole–Cole diagram (*c*). 20 measurement points per decade (only a few points are shown).

that is located in the kilohertz range. This process, connected with the glass transition is the α relaxation already described.

The second (high frequency) mechanism is concerned with the rotation of the OCH_3 group. The maximum amplitude of this motion in the isotropic phase is 0·8. This intramolecular rotation is due to the contribution of the lateral component of the

dipole moment of the alkoxy end group (μ_t). We shall call this process the γ_2 relaxation. A similar high frequency intramolecular rotation has already been observed in low molecular weight mesogens at a frequency one order of magnitude higher [13 (b)].

$E \perp n$. When the electric field is perpendicular to the director, a broad dispersion domain appears, which divides in two parts as the temperature is decreased (see figure 12). The higher frequency domain is connected with the rotation of the OCH_3 group (due to the contribution of μ_t). Its amplitude is large because $\mu_t \gg \mu_1$. Here ε''_{max} is equal to 0·75 in the mesomorphic phase. It is obvious that this motion takes place in the same frequency range for a given temperature as that observed in the parallel measurement direction. The lower frequency domains is the already well-known α relaxation. Below T_g the γ_2 process remains and varies almost independently of temperature. In figure 13 we have reported the variation of the critical frequencies as a function of reciprocal temperature for polymers PLBP29 and PLBP30.
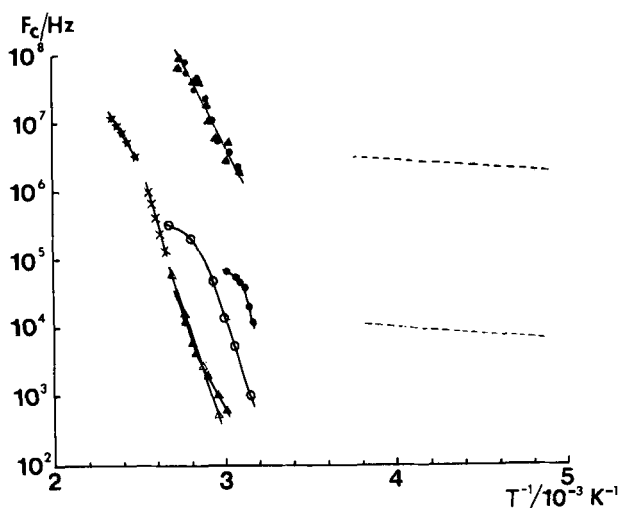

Figure 13.   Critical frequencies against T^{-1} for polymers PLB30 and PLBP ... PLBP30: iso (★); $E \parallel n$ (▲); $E \perp n$ (●); glassy (- - -). PLBP 29: iso (×); $E \parallel n$ (△); $E \perp n$ (○).

In the kilohertz range the relaxation that takes place 60°C above T_g divides in two parts and the motion inside the $(CH_2)_6$ group (β relaxation) is displayed (see figure 13). The amplitude of the β process is very small ($\varepsilon''_{max} = 0·02$). The activation energies of the various processes quoted in various phases of PLBP30 are given in table 2.

We conclude this part by recalling the following points:

(*a*) The δ relaxation is much smaller in amplitude for a polymer with an alkoxy terminal group than with a strong polar cyano terminal group, due to the small value of the longitudinal component (μ_1) of the dipole moment.

(*b*) The α relaxation is displayed in both of the measurement directions but remains more marked when the electric field is perpendicular to the director.

(*c*) The rotational motion of the alkoxy terminal group (γ_2 relaxation) involves the contribution of the transverse component (μ_t) of the resulting dipole moment in both of the main orientations of the director.

(*d*) The mechanism involved in the $-(CH_2)_6-$ section (β relaxation) is very apparent with the alkoxy terminal group and separates easily from the α relaxation when the measurement temperature decreases.

All the molecular motions are frozen at about $100°C$ below the glass transition temperature and the permittivity is equal to $2 \cdot 7$ at $-170°C$ for almost all the polymers investigated.

References

[1] SAMULSKI, E. T., 1982, *Physics Today*, 40.
[2] SHIBAEV, V. P., KOSTROMIN, S. G., PLATE, N. A., IVANOV, S. A., VETROV, V. YU., and YAKOVLEV, Y. A., 1983, *Polym. Commun.*, **24**, 364.
[3] CHOY, C. L., TSE, Y. K., TSUI, S. M., and HSU, B. S. 1974, *Polymer*, **16**, 501.
[4] (a) WILLIAMS, G., 1979, *Advances in Polymer Science*, Vol. 33 (Springer-Verlag). (b) WILLIAMS, G., 1982, *Static and Dynamic Properties of the Polymeric Solid State*, edited by R. A. Dethrick and R. W. Richards, pp. 213–219. (c) HEDVIG, P., 1977, *Dielectric Spectroscopy of Polymers* (Adam Hilger).
[5] KRESSE, H., KOSTROMIN, S., and SHIBAEV, V. P., 1982, *Macromol. Chem. rap. Commun.*, **3**, 509.
[6] KRESSE, H., and TALROZE, R. V., 1981, *Macromol. Chem., rap. Commun.*, **2**, 369.
[7] RINGSDORF, H., STROBL, G., AND ZENTEL, R., 1982, *12 Freiburger Arbeitstagung Flussig-kristalle*, 31.3-2-4.
[8] (a) LEGRAND, C., PARNEIX, J. P., CHAPOTON, A., TINH, N. H., and DESTRADE, C., 1985, *Molec. Crystals liq. Crystals*, **124**, 277. (b) NOËL, C., 1985, *Recent Advances in Liquid Crystalline Polymers*, edited by L. L. Chapoy (Elsevier).
[9] LE BARNY, P., DUBOIS, J. C., FRIEDRICH, C., and NOËL, C., *Polym. Bull.* (to be published).
[10] DRUON, C., 1984, Thesis, Lille.
[11] LIPPENS, D., PARNEIX, J. P., and CHAPOTON, A., 1977, *J. Phys., Paris*, **38**, 1465.
[12] (a) ZENTEL, R., STROBL, G. R., and RINGSDORF, H., 1985, *Macromolecules*, **18**, 960. (b) HAASE, W., PRANOTO, H., and BORMUTH, F. J. 1985, *Ber. Bunsenges. phys. Chem*, **89**, 1229. (c) ATTARD, G. S., and WILLIAMS, G. 1986, *Polym. Commun.*, **27**, 2, 5.
[13] (a) LEGRAND, C., PARNEIX, J. P., CHAPOTON, A., TINH, N. H., and DESTRADE, C., 1984, *J. Phys. Lett., Paris.*, **45**, L 283. (b) PARNEIX, J. P., 1982, Thesis, Lille.
[14] O'REILLY, J. M., 1964, *Modern Aspects of the Vitrious State* edited by J. D. Mackenzie (Butterworths). (1964).
[15] MINKIN, V. I., OSIPOV, O. A., and ZHDANOV, Y. A., 1970, *Dipole Moments in Organic Chemistry* (Plenum Press).